Published for SISSA by Springer

Received: October 27, 2024
Revised: January 13, 2025
Accepted: January 24, 2025
Published: February 14, 2025

Finite-volume effects in the δ-regime

Ulf-G. Meißner[a,b,c,d] **Fabian Müller**[a] **and Akaki Rusetsky**[a,c]

[a] *Helmholtz-Institut für Strahlen- und Kernphysik (Theorie) and Bethe Center for Theoretical Physics, Universität Bonn, 53115 Bonn, Germany*
[b] *Institute for Advanced Simulation (IAS-4), Forschungszentrum Jülich, D-52425 Jülich, Germany*
[c] *Tbilisi State University, 0186 Tbilisi, Georgia*
[d] *Peng Huanwu Collaborative Center for Research and Education, Beihang University, Beijing 100191, China*

E-mail: meissner@hiskp.uni-bonn.de, f.mueller@hiskp.uni-bonn.de, rusetsky@hiskp.uni-bonn.de

Abstract: We derive a systematic perturbative expansion for the finite-volume energy spectrum of the non-linear $O(N)$ σ-model in the δ-regime. The violation of the power-counting rules that emerges after the separation of the fast and slow modes is dealt with to all orders by use of the threshold expansion. The known result for the rest-frame energy spectrum up-to-and-including next-to-next-to-leading order is reproduced.

Keywords: Chiral Lagrangian, Effective Field Theories, Lattice Quantum Field Theory

ArXiv ePrint: 2410.17825

https://doi.org/10.1007/JHEP02(2025)092

JHEP02(2025)092

Contents

JHEP02(2025)092

1 Introduction

In his seminal paper [1], Leutwyler has studied the finite-volume excitation spectrum of QCD in the chiral limit. It was demonstrated that a tower of excitations with a zero three-momentum emerges, whose energy in a box of a size L is proportional to L^{-3}. The excitations with such a small energy cannot be treated in perturbation theory. Rather, they are described by the Lagrangian of the quantum-mechanical rigid rotator. Besides these "slow" modes, the pion field in the effective Lagrangian of QCD contains the so-called "fast" modes (the modes having nonzero three-momenta), whose energy is proportional to L^{-1}. These modes are perturbative and can be treated by using the conventional diagrammatic technique.

In the same paper, different regimes of the low-energy expansion of QCD are identified, depending on the values of the quark masses as well as the external parameters L (the size of the three-dimensional box) and T (the temperature). All these expansions are carried out in powers of $1/(FL)^2$, where F denotes the pion decay constant in the chiral limit that defines the hard scale of the theory. Assume that the quark mass is nonzero and let M denote the

pion mass at lowest order (for simplicity, we restrict ourselves to the isospin-symmetric world with two light quarks). If both the temperature T and M are of order of $1/L$, we are in the so-called p-regime, in which the coefficients in the low-energy expansion are functions of ML and LT. For the smaller quark mass, with $M \ll T \sim L^{-1}$ and $F^2M^2L^3/T \sim 1$, the so-called ϵ-regime sets in, with the low-energy expansion rearranged. Finally, the δ-regime is characterized by the counting rules

$$1/L = O(\delta)\,, \qquad T = O(\delta^3)\,, \qquad M = O(\delta^3)\,. \tag{1.1}$$

Here, δ denotes a generic small parameter.

From the above-mentioned cases, the p-regime is the best explored one. A systematic perturbative approach has been formulated in ref. [2] and is routinely used to evaluate finite-volume artifacts in the observables measured on the lattice.[1] The temperature dependence in this regime is studied, for example, in ref. [9]. Furthermore, a systematic perturbative technique, which has to be used in the ϵ-regime, has been also set up in ref. [9]. The subsequent works [10, 11] used this technique to study the temperature and volume dependence of different fundamental characteristics of the effective field theories (EFT) of QCD at low energy, whereas in ref. [12] the same approach has been utilized to calculate the nucleon mass shift in a finite volume and at a finite temperature. The main difference between the calculations in the p- and ϵ-regimes consists in a different treatment of the slow mode. While in the p-regime all modes are treated on equal footing, the global slow mode is singled out in the ϵ-regime. The partition function in this case is given as a group average of an expression, in which the slow mode is removed.

The foundations for the perturbative framework in the δ-regime have been laid, e.g., in refs. [1, 13, 14]. As already mentioned, this regime is relevant for the study of the chiral limit in QCD, see, e.g., the recent work [15], as well as an attempt to determine some of the $O(p^4)$ low-energy constants via the simulations carried out in the δ-regime [16]. Perhaps an even more interesting application of the framework is the study of the volume dependence in different models of condensed matter physics, which feature massless excitations in the spontaneously broken phase. For example, the long-wavelength physics of the undoped antiferromagnets is described by the $O(N)$ non-linear σ-model [17–19]. A perturbative framework for these kind of models, which goes under the name of Magnon Chiral Perturbation Theory, is formally equivalent to the one used to describe QCD in the chiral limit. In the selected papers given below we tried to credit the important work carried out so far in this field [20–30]. Furthermore, it was shown that the hole-doped antiferromagnets with the spontaneously broken SU(2) spin symmetry in the long-wavelength limit are described by the Chiral Perturbation Theory of magnons and holes (massive fermions), in a direct reminiscence of the Baryon Chiral Perturbation Theory [31–36].

Despite the significant effort invested in the study of the δ-regime in the last decades, the formalism used still contains caveats which need to be addressed. Namely, in the p-

[1]The case $ML \gg 1$ and $T \ll M$ can be also attributed to the p-regime. Scattering observables (e.g., two-body scattering phase shifts, weak and electromagnetic decay amplitudes, timelike form factors, etc.) are measured on the lattice in this regime. The Lüscher finite-volume approach [3] has become a standard tool to analyze lattice data on two-particle scattering and a three-particle framework has been recently proposed as well [4–8].

JHEP02(2025)092

and ϵ-regimes, consistent Feynman rules can be written down that enable one to carry out calculations (in principle) to any given order in the expansion. Namely, in the p-regime, a single momentum scale $p \sim 1/L$ is relevant and, hence, the expansion can be carried out without further ado. Furthermore, the global slow mode in the ϵ-regime can be straightforwardly taken into account with the use of the Faddeev-Popov trick. To the contrary, the slow mode in the δ-regime is time-dependent and corresponds to a dynamical degree of freedom, whose energy scales as $1/L^3$ in the chiral limit (we remind the reader that the energies of the fast modes scale as $1/L$, see also a related discussion in ref. [15]). Stated differently, we face a well-known situation of the EFT with two distinct scales that need to be clearly separated in order to yield a consistent framework. In addition, note that the standard Feynman diagrammatical method cannot be used for the slow mode that makes the separation of scales technically challenging, albeit a perturbative expansion of the Green functions still can be carried out. In the literature, one finds examples of calculations of the higher-order corrections [1, 13, 14, 22, 23], originating from the loop corrections with the fast modes alone. However, even if, in some cases, the contribution from the slow mode can be relegated to a rather high order by using a very special field transformation [13, 14], carrying out a systematic expansion to all orders still remains a challenge. The present work aims at closing this gap.

In this paper we shall demonstrate that a consistent perturbative framework in the δ-regime emerges by using the so-called "threshold expansion" in all diagrams containing fast as well as slow modes [37]. In order to set the stage, we shall concentrate on the $O(N)$ σ-model and try to reproduce the result of refs. [13, 14] with the use of the alternative technique proposed here (the generalization to other models is relatively straightforward and will not be considered in this work). It will in particular be demonstrated that the field redefinition introduced in refs. [13, 14] is in fact unnecessary — the threshold expansion neatly does the job (in fact, it is not clear, whether a similar field redefinition can be used in higher orders as well). We would like to stress that we do not aim to obtain new results here, pursuing the calculations to even higher orders. Our aim is rather to set systematic rules that enable carrying out calculations to an arbitrary order without using additional tricks and which could be eventually extended to the case where massive fermions are also present. For clarity, we note that all our calculations will be performed in (split) dimensional regularization. The space extension of a box L is finite and the periodic boundary conditions are imposed in spatial directions. Furthermore, the calculations are performed at zero temperature, i.e., the time extension is assumed to be infinite.

The paper is organized as follows. In section 2 we briefly review the existing approach in case of the $O(N)$ σ-model and write down the path integral representation of the Green functions we want to calculate. The low-lying spectrum at the leading order is considered in the rest-frame as well as moving frames. In section 3 we show that the results of refs. [13, 14] can be reproduced in any field parameterization, provided the threshold expansion is used. Section 4 contains our conclusions and outlook. Various technical details are relegated to the appendices.

JHEP02(2025)092

2 Path integral representation of the Green functions, the finite-volume spectrum and matrix elements

2.1 The Lagrangian and the observables

The (Euclidean) Lagrangian of the $O(N)$ σ-model, which will be used to demonstrate our method, is given by the following expression

$$\mathscr{L} = \mathscr{L}^{(2)} + \mathscr{L}^{(4)} + \cdots . \tag{2.1}$$

The lowest-order (LO) Lagrangian is given by:

$$\mathscr{L}^{(2)} = \frac{F^2}{2}\, \partial_\mu S^\alpha \partial_\mu S^\alpha . \tag{2.2}$$

Here, S^α, $\alpha = 0, 1, \ldots, N-1$, denotes a unit N-component real scalar field that transforms under $O(N)$. Note also that the above Lagrangian does not contain chiral symmetry breaking terms and thus describes exactly massless Goldstone bosons. With a slight abuse of language, we shall call these particles "pions" for brevity.

At next-to-leading order (NLO) two additional terms arise that contain the low-energy constants ℓ_1, ℓ_2:

$$\mathscr{L}^{(4)} = -\ell_1 (\partial_\mu S^\alpha \partial_\mu S^\alpha)(\partial_\nu S^\beta \partial_\nu S^\beta) - \ell_2 (\partial_\mu S^\alpha \partial_\nu S^\alpha)(\partial_\mu S^\beta \partial_\nu S^\beta) . \tag{2.3}$$

All information about the observables is encoded in the Green functions of the field $S^\alpha(x)$. For example, the single-particle spectrum in a finite volume can be extracted from the two-point function in the following manner. Following ref. [38], in the rest-frame we consider the correlator[2]

$$C(t) = \frac{1}{L^6} \int d^3\boldsymbol{x}\, d^3\boldsymbol{y}\, \langle S^\alpha(x) S^\alpha(y) \rangle , \qquad t = x_0 - y_0 . \tag{2.4}$$

Here, the integration over the spatial dimensions projects onto the states with the zero total three-momentum and is carried out in a finite cube. For large Euclidean time separations, one has[3]

$$C(t) = \text{const} \cdot e^{-M(L)t} + O\left(\exp\left(-\frac{4\pi t}{L}\right)\right) . \tag{2.5}$$

It is tempting to interpret $M(L)$ as the pion "mass" in a box of size L. This interpretation comes, however, with a grain of salt, see below.

Furthermore, in the theory described by the Lagrangian (2.1), the correlator can be expanded in regular perturbation series, where the quantity $1/(FL)^2$ plays the role of the small parameter

$$C(t) = 1 + \sum_{i=0}^{\infty} \frac{1}{(FL)^{2(i+1)}}\, C_i\left(\frac{t}{L}\right) . \tag{2.6}$$

[2] On the lattice as explained in ref. [38], one should impose free boundary conditions in the time direction. This ensures that the states corresponding to the different excited levels of the rigid rotator do not mix. In our analytic calculations the time elongation of the lattice is taken to be infinite.

[3] The suppression factor of the remainder in eq. (2.5) will be justified below, see section 2.4.

JHEP02(2025)092

Anticipating that $M(L)$ scales like $1/(F^2L^3)$, we expand the first term in the correlator in powers of $M(L)t$ (the remainder is still exponentially suppressed, since $t/L \sim 1$ is assumed). Comparing this expansion with eq. (2.6), one may further conclude that the coefficients of the expansion are polynomials in t/L:

$$C_i\left(\frac{t}{L}\right) = \sum_{k=0}^{i+1} C_{ik}\left(\frac{t}{L}\right)^k + O\left(\exp\left(-\frac{4\pi t}{L}\right)\right). \tag{2.7}$$

From eq. (2.5) it is also seen that the expansion of $\ln C(t)$ should be linear in t and the higher-order terms must cancel. The coefficient in front of the linear term determines $M(L)$, whereas the cancellation of the higher-order terms provides a useful check in the calculations.

Furthermore, one could try to generalize the above method to moving frames with arbitrary three-momentum $\boldsymbol{p}$. The counterpart of eq. (2.4) reads

$$C(t,\boldsymbol{p}) = \frac{1}{L^6}\int d^3\boldsymbol{x}\, d^3\boldsymbol{y}\, e^{-i\boldsymbol{p}(\boldsymbol{x}-\boldsymbol{y})}\langle S^\alpha(x)S^\alpha(y)\rangle\,. \tag{2.8}$$

The behavior of the correlation function at large values of t is given by

$$C(t,\boldsymbol{p}) = \text{const}\cdot e^{-E(L,\boldsymbol{p})t} + \cdots\,, \tag{2.9}$$

where the ellipses stand for the exponentially suppressed contributions.

In moving frames, the ground-state energy $E(L,\boldsymbol{p})$ scales as $1/L$, and so does the energy gap between the ground state and the lowest excited level. The logarithm of $C(t,\boldsymbol{p})$ will still be a linear function of t up to exponential corrections. One could use this property and drop these exponential corrections "by hand". In the remainder, the energy $E(L,\boldsymbol{p})$ is still given by the coefficient in the linear term. Finally, a similar method can be applied for extracting the k-pion energy levels (both in the center-of-mass and moving frames). The simplest way to achieve this is to use a product of k pion fields $O^{\alpha_1\cdots\alpha_k}(x) = S^{\alpha_1}(x)\cdots S^{\alpha_k}(x)$. From $O^{\alpha_1\cdots\alpha_k}(x)$ one could construct a traceless fully symmetric tensor by subtracting traces with respect to each pair of indices. This tensor transforms as a basis vector of an irreducible representation of $O(N)$, which is not contained in the product of m fundamental representations for any $m < k$. Other observables, like the magnetization and susceptibility, can also be expressed in terms of the Green functions and evaluated in perturbation theory in a form of a regular expansion in $1/(FL)^2$.

The main challenge that emerges in the construction of the perturbative series in $1/(FL)^2$ is the emergence of the so-called slow mode (or, zero mode), which leads to the ill-defined terms in standard Feynman diagrams. In order to arrive at the Feynman diagrams without singularities, the contribution of the slow mode should be treated separately from the rest. In the following section, we shall briefly discuss how this goal should be achieved.

2.2 Separation of the slow modes

The technique for the removal of the slow mode is well known in the literature, see, e.g., [13, 14, 22]. In order to keep the presentation self-contained, we shall briefly recapitulate crucial points of the derivation below. The collective coordinate, corresponding to the time-dependent

JHEP02(2025)092

net magnetization $m^\alpha(t)$, will be singled out by using the Faddeev-Popov trick.[4] To this end, we insert the following identity into the path integral

$$1 = \prod_t \int d^N m(t) \prod_{\alpha=0}^{N-1} \delta\left(m^\alpha(t) - \frac{1}{L^3} \int d^3\boldsymbol{x}\, S^\alpha(\boldsymbol{x},t)\right) . \tag{2.10}$$

Next, one defines the unit vector $e^\alpha(t)$, and

$$m^\alpha(t) = m(t)e^\alpha(t)\,, \qquad d^N m(t) = m^{N-1}(t)dm(t)d^N e(t)\,\delta\left(e^\alpha(t)e^\alpha(t)-1\right) . \tag{2.11}$$

The partition function can be rewritten as follows

$$\begin{aligned} Z &= \prod_x \int d^N S(x)\delta\left(S^\alpha(x)S^\alpha(x)-1\right)\exp\left(-A\left[S\right]\right) \\ &= \prod_x \int d^N S(x)\delta\left(S^\alpha(x)S^\alpha(x)-1\right)\prod_t \int m^{N-1}(t)dm(t)d^N e(t)\,\delta\left(e^\alpha(t)e^\alpha(t)-1\right) \\ &\quad \times \delta^N\left(m(t)e^\alpha(t) - \frac{1}{L^3}\int d^3\boldsymbol{x}\, S^\alpha(\boldsymbol{x},t)\right)\exp\left(-A\left[S\right]\right) , \end{aligned} \tag{2.12}$$

where

$$A\left[S\right] = \int d^4x \mathscr{L}\left[S(x)\right] \tag{2.13}$$

denotes the action functional. We further define the $O(N)$ rotation matrix $\Omega(t)$ as

$$e^\alpha(t) = \Omega^{\alpha\beta}(t)n^\beta\,, \qquad n = (1,0,\ldots,0)\,, \tag{2.14}$$

and choose the following parameterization of $\Omega(t)$

$$\begin{aligned} &\Omega^{00}(t) = e^0(t), \qquad \Omega^{i0}(t) = e^i(t)\,, \qquad \Omega^{0i}(t) = -e^i(t)\,, \\ &\Omega^{ij}(t) = \delta^{ij} - \frac{e^i(t)e^j(t)}{1+e^0(t)}\,, \qquad i,j = 1,\ldots,N-1\,. \end{aligned} \tag{2.15}$$

Introducing now the new variable $S^\alpha(x) = \Omega^{\alpha\beta}(t)R^\beta(x)$, the partition function can be rewritten as[5]

$$\begin{aligned} Z &= \prod_x \int d^N R(x)\delta\left(R^\alpha(x)R^\alpha(x)-1\right)\prod_t \int m^{N-1}(t)dm(t)d^N e(t)\,\delta\left(e^\alpha(t)e^\alpha(t)-1\right) \\ &\quad \times \delta^N\left(m(t)n^\alpha - \frac{1}{L^3}\int d^3\boldsymbol{x}\, R^\alpha(\boldsymbol{x},t)\right)\exp\left(-A\left[\Omega R\right]\right) . \end{aligned} \tag{2.16}$$

[4] In the ϵ-regime, with $L \sim T^{-1}$, the net magnetization m^α is a constant. For $T^{-1} \gg L$, however, this approximation is no more valid and the time-dependent $m^\alpha(t)$ corresponds to a dynamical degree of freedom.

[5] The matrix $\Omega(t)$ is not defined unambiguously, since the vector n is invariant under $O(N-1)$ group transformations in the subspace orthogonal to it. This property was used in refs. [13, 14, 22], where the variable transformation in the path integral was written down as $S^\alpha(x) = \left(\Omega(t)\Sigma^T(t)\right)^{\alpha\beta} R^\beta(x)$. The block-diagonal matrix $\Sigma^T(t)$, which leaves the vector n invariant, was chosen in a particular form that enabled to significantly simplify the structure of the Lagrangian at the order one is working. In our paper, we do not resort to such a field redefinition and reproduce the result of the above-mentioned papers by applying the threshold expansion in all relevant Feynman integrals.

JHEP02(2025)092

Here, the invariance of the δ-function with respect of the $O(N)$ group transformations has been used. Next, choosing the parameterization $R = (R^0, \boldsymbol{R}) \doteq (\sqrt{1-\boldsymbol{R}^2}, \boldsymbol{R})$, and carrying out the integration over the variables $R^0(x)$ and $m(t)$, we get

$$Z = \prod_x \int d\boldsymbol{R}(x) \prod_t \int d^N e(t)\, \delta\left(e^\alpha(t) e^\alpha(t) - 1\right)\, J \\ \times \delta^{N-1}\left(-\frac{1}{L^3}\int d^3\boldsymbol{x}\, \boldsymbol{R}(\boldsymbol{x}, t)\right) \exp\left(-A\left[\Omega R\right]\right) . \tag{2.17}$$

Here, the factor J is given by

$$J = \prod_x \frac{1}{2\sqrt{1-\boldsymbol{R}^2(x)}} \times \prod_t \left(\frac{1}{L^3}\int d^3\boldsymbol{x}\, \sqrt{1-\boldsymbol{R}^2(x)}\right)^{N-1} \\ = \text{const} \cdot \exp\left(-\delta^4(0)\int d^4x \ln\sqrt{1-\boldsymbol{R}^2(x)}\right. \\ \left. + (N-1)\,\delta(0)\int dt \ln\left(\frac{1}{L^3}\int d^3\boldsymbol{x}\sqrt{1-\boldsymbol{R}^2(x)}\right)\right) . \tag{2.18}$$

It is seen that the argument of the exponent vanishes in dimensional regularization.[6] For this reason, we shall set the factor J equal to one in the following (the physical results, of course, do not depend on the regularization used). Note that the path integral representation for a generic Green function looks similar to eq. (2.17) — in this case the integrand, in addition, contains the product of the pertinent operators, expressed in terms of the variables $\boldsymbol{R}(x)$ and $e^\alpha(t)$. The latter correspond to the fast and slow modes, respectively. The representation displayed in eq. (2.17) provides the basis for the perturbative expansion of the Green function in powers of $1/L$ (modulo logarithms).

2.3 Expansion of the Lagrangian

In order to formulate the Feynman rules, one has to expand the Lagrangian and separate the "free" part from the rest. The expansion proceeds along the standard pattern and the "free" Lagrangian is given by

$$\mathscr{L}_{\mathsf{free}} = \frac{F^2}{2}\,\dot{e}^\alpha(t)\dot{e}^\alpha(t) + \frac{F^2}{2}\,\partial_\mu \boldsymbol{R}(x)\partial_\mu \boldsymbol{R}(x)\,. \tag{2.19}$$

The above Lagrangian represents a sum of the Lagrangian of the rigid rotator and the free massless field Lagrangian. In the latter, the mode with zero three-momentum is absent. All other terms obtained in the expansion of the full Lagrangian in powers of $\boldsymbol{R}$ are considered as a perturbation. Note that a rigid rotator does not describe non-interacting particles in the standard sense. This was the reason for putting the word "free" in quotation marks.

The two-point function of the free fast fields is given by

$$\langle R^i(x) R^j(y)\rangle = \frac{\delta^{ij}}{F^2}\int \frac{dk_0}{2\pi}\,\frac{1}{L^3}\sum_{\boldsymbol{k}\neq 0}\frac{e^{ik(x-y)}}{k_0^2+\boldsymbol{k}^2} \doteq \frac{\delta^{ij}}{F^2}\,d(x-y)\,. \tag{2.20}$$

[6] In order to arrive at this conclusion, one has to use the so-called split dimensional regularization, i.e., regularize the timelike $\tau = 1+\varepsilon'$ and spacelike $d = 3+\varepsilon$ dimensions separately, with $D = d+\tau$ and $\varepsilon, \varepsilon' \to 0$ at the end [39]. The quantities $\delta^4(0)$ and $\delta(0)$ in eq. (2.18) are replaced by $\delta^D(0)$ and $\delta^\tau(0)$ which vanish in dimensional regularization.

JHEP02(2025)092

Both the energy k_0 and the three-momentum $\boldsymbol{k}$ count as $1/L$. Note also that the above sum does not contain the zero three-momentum term $\boldsymbol{k} = 0$. These terms are singled out and are described by the slow mode.

The slow mode $e^\alpha(t)$ depends on the time only. Its three-momentum is exactly zero, and its energy counts as $1/L^3$. Thus, one anticipates the breaking of the power counting through the loops which contain both fast and slow momenta. The exact two-point function of the slow fields can easily be written down. However, it is not very useful since Wick's theorem for the slow fields cannot be used, owing to the fact that the free Lagrangian for the slow modes coincides with the one of a rigid rotator and not of a harmonic oscillator (see also appendix A).

In the following, we plan to carry out the perturbative expansion step by step and identify the place where the counting rule breaks down. In order to set the stage, we shall focus exclusively on the calculation of the one-particle spectrum.

2.4 Two-point function at the lowest order

We start from the two-point function at lowest order which nicely factorizes:

$$\begin{aligned} C(x-y) &= \langle S^\alpha(x) S^\alpha(y)\rangle \\ &= \langle \Omega^{\alpha 0}(x^0)\Omega^{\alpha 0}(y^0)\rangle \langle R^0(x) R^0(y)\rangle \\ &\quad + \langle \Omega^{\alpha i}(x^0)\Omega^{\alpha 0}(y^0)\rangle \langle R^i(x) R^0(y)\rangle \\ &\quad + \langle \Omega^{\alpha 0}(x^0)\Omega^{\alpha i}(y^0)\rangle \langle R^0(x) R^i(y)\rangle \\ &\quad + \langle \Omega^{\alpha i}(x^0)\Omega^{\alpha j}(y^0)\rangle \langle R^i(x) R^j(y)\rangle \,. \end{aligned} \tag{2.21}$$

In this expression, the vacuum expectation values of the slow and fast variables are defined as follows

$$\begin{aligned} \langle \Omega^{\alpha\beta}(x^0)\Omega^{\gamma\delta}(y^0)\cdots\rangle &= \prod_t \int d^N e(t)\delta(e^\lambda(t)e^\lambda(t)-1)\left(\Omega^{\alpha\beta}(x^0)\Omega^{\gamma\delta}(y^0)\cdots\right) \\ &\quad \times \exp\left(-\frac{F^2L^3}{2}\int dt\, \dot e^\sigma(t)\dot e^\sigma(t)\right), \\ \langle R^\alpha(x)R^\beta(y)\cdots\rangle &= \prod_x \int d\boldsymbol{R}(x)\delta^{N-1}\left(-\frac{1}{L^3}\int d^3\boldsymbol{x}\, \boldsymbol{R}(\boldsymbol{x},t)\right) \\ &\quad \times \left(R^\alpha(x)R^\beta(y)\cdots\right)\exp\left(-\frac{F^2}{2}\int d^4x \partial_\mu \boldsymbol{R}(x)\partial_\mu \boldsymbol{R}(x)\right). \end{aligned} \tag{2.22}$$

The second and the third terms in eq. (2.21) vanish identically, because the free Lagrangian has the symmetry with respect to $\boldsymbol{R}\to -\boldsymbol{R}$. The fast mode propagator in the fourth term is given in eq. (2.20), whereas the correlator of two composite fields R^0 in the first term can be expanded as

$$\begin{aligned} \langle R^0(x)R^0(y)\rangle &\doteq T_0(x-y) \\ &= 1 - \langle \boldsymbol{R}^2(0)\rangle - \frac{1}{4}\langle\left(\boldsymbol{R}^2(0)\right)^2\rangle + \frac{1}{4}\langle \boldsymbol{R}^2(x)\boldsymbol{R}^2(y)\rangle + O(\boldsymbol{R}^6) \\ &= 1 - \frac{N-1}{F^2}\,d(0) - \frac{N-1}{2F^4}\,d^2(0) + \frac{N-1}{2F^4}\,d^2(x-y) + O(F^{-6}) \\ &\doteq \sum_{a=0}^{\infty} C_a d^{2a}(x-y)\,. \end{aligned} \tag{2.23}$$

Performing the Fourier transform, one gets

$$\begin{aligned} C(t,\boldsymbol{p}) &\doteq \int d^3\boldsymbol{x} e^{-i\boldsymbol{p}\boldsymbol{x}} C(x) \\ &= \langle \Omega^{\alpha i}(t)\Omega^{\alpha i}(0)\rangle \frac{1-\delta_{\boldsymbol{p}0}}{F^2}\,\frac{e^{-|\boldsymbol{p}|t}}{2|\boldsymbol{p}|} \\ &\quad + \langle \Omega^{\alpha 0}(t)\Omega^{\alpha 0}(0)\rangle \int d^3\boldsymbol{x} e^{-i\boldsymbol{p}\boldsymbol{x}} T_0(\boldsymbol{x},t)\,. \end{aligned} \tag{2.24}$$

In this expression,

$$\begin{aligned} \int d^3\boldsymbol{x} e^{-i\boldsymbol{p}\boldsymbol{x}} T_0(\boldsymbol{x},t) = L^3\delta_{\boldsymbol{p}0} + \sum_{a=1}^{\infty} \frac{C_a}{L^{6a}} \sum_{\boldsymbol{k}_1\cdots\boldsymbol{k}_{2a}} L^3\delta_{\boldsymbol{p},\boldsymbol{k}_1+\cdots+\boldsymbol{k}_{2a}} \\ \times (1-\delta_{\boldsymbol{k}_1 0})\cdots(1-\delta_{\boldsymbol{k}_{2a}0}) \frac{\exp(-(|\boldsymbol{k}_1|+\cdots+|\boldsymbol{k}_{2a}|)t)}{2|\boldsymbol{k}_1|\cdots 2|\boldsymbol{k}_{2a}|}\,. \end{aligned} \tag{2.25}$$

We consider two cases separately:

- $\boldsymbol{p}=0$. In this case, the first term in eq. (2.24) does not contribute. Furthermore, in the momentum sums contained in the quantity T_0, see eq. (2.25), one always has $|\boldsymbol{k}|_1+\cdots+|\boldsymbol{k}|_{2a}\geq 2$ (in units of $2\pi/L$). Hence, the leading contribution comes from the constant term, and we get:

$$C(t,\boldsymbol{0}) = L^3\langle \Omega^{\alpha 0}(t)\Omega^{\alpha 0}(0)\rangle + O\left(\exp\left(-\frac{4\pi}{L}\right)\right)\,. \tag{2.26}$$

  Note that the argument of the exponentially suppressed term was already anticipated in eq. (2.5).

- $\boldsymbol{p}\neq 0$. In this case, the first term in eq. (2.24) contributes. Furthermore, $|\boldsymbol{k}|_1+\cdots+|\boldsymbol{k}|_{2a}\geq|\boldsymbol{p}|$ always holds for $\boldsymbol{k}_1+\cdots+\boldsymbol{k}_{2a}=\boldsymbol{p}$ and $\boldsymbol{k}_i\neq 0$. Note that for $|\boldsymbol{p}|\geq 2$ the configurations of $\boldsymbol{k}_i$ exist that obey the equality $|\boldsymbol{k}|_1+\cdots+|\boldsymbol{k}|_{2a}=|\boldsymbol{p}|$. We denote the sum over such configurations by $\sum'$. For all other configurations, $|\boldsymbol{k}|_1+\cdots+|\boldsymbol{k}|_{2a}\geq|\boldsymbol{p}|+a$, where a depends on the choice of the vector $\boldsymbol{p}$. Hence, we have:

$$\begin{aligned} C(t,\boldsymbol{p}) &= \langle \Omega^{\alpha i}(t)\Omega^{\alpha i}(0)\rangle \frac{e^{-|\boldsymbol{p}|t}}{2F^2|\boldsymbol{p}|} + \langle \Omega^{\alpha 0}(t)\Omega^{\alpha 0}(0)\rangle e^{-|\boldsymbol{p}|t} \\ &\quad \times \left(\sum_a \frac{C_a}{L^{6a}} \sum_{\boldsymbol{k}_1\cdots\boldsymbol{k}_{2a}}{}' \frac{L^3\delta_{\boldsymbol{p},\boldsymbol{k}_1+\cdots+\boldsymbol{k}_{2a}}(1-\delta_{\boldsymbol{k}_1 0})\cdots(1-\delta_{\boldsymbol{k}_{2a}0})}{2|\boldsymbol{k}_1|\cdots 2|\boldsymbol{k}_{2a}|} + O(e^{-at})\right). \end{aligned} \tag{2.27}$$

Furthermore, in order to evaluate the vacuum expectation value of the product of two Ω's, we insert a full set of the rigid rotator eigenstates between two operators

$$\begin{aligned} \langle \Omega^{\alpha i}(t)\Omega^{\alpha i}(0)\rangle &= \sum_n e^{-\varepsilon_n t}\langle 0|\Omega^{\alpha i}(0)|n\rangle\langle n|\Omega^{\alpha i}(0)|0\rangle\,, \\ \langle \Omega^{\alpha 0}(t)\Omega^{\alpha 0}(0)\rangle &= \sum_n e^{-\varepsilon_n t}\langle 0|\Omega^{\alpha 0}(0)|n\rangle\langle n|\Omega^{\alpha 0}(0)|0\rangle\,. \end{aligned} \tag{2.28}$$

JHEP02(2025)092

Here,

$$\varepsilon_n = \frac{n(n+N-2)}{2\Theta}\,, \qquad n = 0, 1, \ldots \tag{2.29}$$

denotes the n^{th} eigenvalue of the Hamiltonian, corresponding to the eigenvector $|n\rangle$ and $\Theta = F^2L^3$ is the moment of inertia. As seen, the eigenvalues scale as L^{-3}.

In the next step, we consider the sums over the eigenvectors of the rigid rotator (more details can be found in appendix B). Since $\Omega^{\alpha 0} = e^\alpha$ is the irreducible tensor operator belonging to the fundamental representation of $O(N)$, all matrix elements $\langle 0|\Omega^{\alpha 0}(0)|n\rangle$ vanish except for $n = 1$. Furthermore, using a proper choice of the basis vectors in the fundamental representation, $|1,\gamma\rangle\,,\ \gamma = 1,\ldots,N$, the above matrix element takes a simple form $\langle 0|\Omega^{\alpha 0}(0)|1\gamma\rangle = \delta^{\alpha\gamma}$ (the normalization of the matrix follows from the condition $e^\alpha e^\alpha = 1$). The calculation of the matrix element of $\Omega^{\alpha i}$ is a more complicated task and is considered in appendix B). Here, it suffices to say that the state with $n = 0$ also contributes to the sum over the intermediate states since the corresponding matrix element does not vanish.

To summarize, the free finite-volume spectrum of the two-point function has rather peculiar properties. Namely, in the rest-frame, the lowest excitation has the energy $\varepsilon_1(L) = (N-1)/(2F^2L^3)$ and the first excited level is separated by $4\pi/L$. In the frame moving with a momentum $\boldsymbol{p}$, the lowest energy level is exactly at $E = |\boldsymbol{p}|$. This, by the way, demonstrates that interpreting the quantity $(N-1)/(2F^2L^3)$ as the pion mass in a finite volume is a slight abuse of language, because the lowest level in different frames does not obey the relativistic dispersion law. This does not come at a complete surprise, since the separation of the fast and slow modes is done in the rest-frame and breaks Lorentz invariance from the beginning. In case of massive particles, there exists a natural scale: if $ML \gg 1$, the fast and slow modes glue together and form a relativistic particle. There exists no such scale in the massless case and the lattice breaks relativistic invariance at all scales.

2.5 Perturbative expansion

At the next step, we evaluate radiative corrections to the two-point function, in order to obtain a regular expansion of the low-lying spectrum in powers of $1/(FL)^2$. At NLO, it suffices to work with the Lagrangian $\mathscr{L}^{(2)}$. Expanding this Lagrangian in powers of the field $\boldsymbol{R}$, one gets:

$$\mathscr{L}^{(2)} = \mathscr{L}_{\text{free}} - \frac{F^2}{2}\,\dot{e}^\alpha \dot{e}^\alpha \boldsymbol{R}^2 + \frac{F^2}{2}\,\dot{\Omega}^{\alpha i}\dot{\Omega}^{\alpha j} R^i R^j + \frac{F^2}{2}\,\left(\dot{\Omega}^{\alpha i}\Omega^{\alpha j} - \dot{\Omega}^{\alpha j}\Omega^{\alpha i}\right) R^i \dot{R}^j + \cdots\,. \tag{2.30}$$

At this place, it is appropriate to discuss the power counting. The dimensionless field $e^\alpha(t)$ counts as $O(1)$. From eq. (2.20) one concludes that the field $\boldsymbol{R}(x)$ should count as $O(L^{-1})$ (we remind the reader that all components of the four-momentum of the fast mode count as $O(L^{-1})$). On the contrary, the energy of the soft mode counts as $O(L^{-3})$, and its three-momentum is zero by definition. Consequently, $\dot{e}^\alpha(t)$ in the Lagrangian counts as $O(L^{-3})$ and $\partial_\mu \boldsymbol{R}(x)$ as $O(L^{-2})$. The free Lagrangian of the slow modes, which will be used to read off the spectrum, is given in eq. (2.19) and counts as $O(L^{-6})$. This effective Lagrangian is obtained by integrating out the fast modes. To this end, one first writes:

$$\begin{aligned}\exp\left(-\int d^4x\,\mathscr{L}^{(2)}(x)\right) = 1 - \frac{1}{1!}\int d^4x\,\mathscr{L}^{(2)}(x) \\ + \frac{1}{2!}\int d^4x\,\mathscr{L}^{(2)}(x)\int d^4y\,\mathscr{L}^{(2)}(y) + \cdots\,,\end{aligned} \tag{2.31}$$

JHEP02(2025)092

integrates out the fields $\boldsymbol{R}(x)$ in the path integral and finally exponentiates the remainder back. Dealing with the first two terms is easy: in the first-order term of eq. (2.31) we have two fields $R^i(x)R^j(x)$ which have to be contracted. This is equivalent to replacing $R^i(x)R^j(x)$ by $\langle R^i(x)R^j(x)\rangle$ in the Lagrangian. Graphically, this corresponds to the tadpole diagram shown in figure 1a. It is immediately seen that the resulting term in the Lagrangian should count as $O(L^{-8})$ and thus results into a $O(L^{-2})$ correction to the leading-order result for the energy spectrum. Higher order terms in perturbation theory (2.31) with this part of the Lagrangian will be more suppressed and are not considered here. With the last term in eq. (2.30), the situation is slightly different. The tadpole term does not contribute, because $\langle \dot{R}^i(x)R^j(x)\rangle = 0$. Integrating out the fields $\boldsymbol{R}(x)$ in the second-order term of eq. (2.31) leads to a loop shown in figure 1b. In addition of the product of four fields Ω with two time derivatives that count as $O(L^{-6})$, there are two additional lines of field $\boldsymbol{R}(x)$, two derivatives on these fields and an additional integration over d^4x. All this results in a factor $O(L^{-2})$ in addition, so the contribution of the diagram figure 1b in the effective Lagrangian counts as $O(L^{-8})$, the same as the contribution of figure 1a. We would also stress here that the whole discussion above is based on the naive power counting which gives the leading power correctly.

In refs. [13, 14, 22], a field transformation in the Lagrangian given by eq. (2.30) is performed that renders its structure simpler. We discuss this transformation in detail in appendix C. It has the following structure

$$\Omega(t) \to \Omega(t)\Sigma^T(t)\,, \tag{2.32}$$

where

$$\Sigma^{00}(t) = 1\,, \qquad \Sigma^{0j}(t) = \Sigma^{i0}(t) = 0\,, \qquad \Sigma^{ij}(t) = \hat{\Sigma}^{ij}(t)\,, \tag{2.33}$$

and $\hat{\Sigma}(t) \in O(N-1)$. Clearly, this transformation leaves the vector $n = (1, 0, \ldots, 0)$ invariant, see footnote 5.

It can be shown (see appendix C) that, after the field transformation with a properly chosen matrix Σ, the last term in eq. (2.30) vanishes:

$$\frac{d}{dt}\,(\Omega(t)\Sigma^T(t))^{\alpha i}(\Omega(t)\Sigma^T(t))^{\alpha j} = 0\,. \tag{2.34}$$

Furthermore, it can be shown that, after the same transformation,

$$\frac{d}{dt}\,(\Omega\Sigma^T)^{\alpha i}(t)\frac{d}{dt}\,(\Omega\Sigma^T)^{\alpha i}(t) = \frac{1}{2}\,\dot{e}^\alpha(t)\dot{e}^\alpha(t)\,. \tag{2.35}$$

This allows one to use a shortcut in the calculation of the excitation spectrum at NLO. At this order, only the tadpole diagrams shown in figure 1a contribute, and the net effect reduces to a correction to the moment of inertia

$$\Theta \to \Theta\Big(1 - \frac{N-2}{F^2}\,d(0)\Big)\,. \tag{2.36}$$

The excitation spectrum in the rest-frame is given by [14]

$$\varepsilon_n = \frac{n(n+N-2)}{2F^2L^3}\left(1 + \frac{N-2}{F^2}\,d(0)\right),\ n = 0, 1, \ldots \tag{2.37}$$

JHEP02(2025)092

Note that, according to eq. (2.20), the quantity $d(0)$ is of order $1/L^2$. No multi-scale integrals arise, and the power counting is not violated. Furthermore, as shown in ref. [14], no new structures arise at NNLO as well, and hence the same method can be used for calculations also in this case.[7] It, however, remains unclear how this field transformation can be systematically performed at higher orders. On the other hand, physical results cannot depend on the choice of the interpolating field. This is not immediately manifest in the present example. If the field transformation is not performed, the loop diagram (the self-energy) shown in figure 1b also contributes. The integrand of this diagram depends on different low-energy scales, and the power counting is not straightforward. In the following section we shall demonstrate how the above problems can be addressed.

3 The threshold expansion

3.1 NLO

As became clear from the previous discussion, the main problem that precludes carrying out a systematic expansion in inverse powers of L is related to the presence of different scales in the Feynman diagrams. A standard method to address this problem, applicable at any order, is to use threshold expansion in these diagrams. This method enables one to arrive at the final result without further ado (e.g., field redefinitions). The independence of the result on the choice of the field will then represent a nice test of the calculations.

We shall first explain this method in detail at NLO. Since we focus on the calculation of the excitation spectrum in the rest frame, we shall use the same shortcut as in refs. [13, 14, 22], evaluating the (non-local) effective action at second order. The piece of this action that contains the contribution of the diagram in figure 1b (the culprit) to the pion self-energy, is given by

$$\delta S_{\mathsf{eff}}^{(b)} = \int d^4x\, \delta\mathscr{L}_{\mathsf{eff}}^{(b)}(x)\,, \tag{3.1}$$

where

$$\delta\mathscr{L}_{\mathsf{eff}}^{(b)}(x) = -\frac{F^4}{8}\int d^4z \Lambda^{ij}(u_0)\Lambda^{kn}(v_0)\Big(\langle R^i(u)R^k(v)\rangle\langle\dot{R}^j(u)\dot{R}^n(v)\rangle + \langle R^i(u)\dot{R}^n(v)\rangle\langle\dot{R}^j(u)R^k(v)\rangle\Big)\,. \tag{3.2}$$

Here, $u = x + z/2$, $v = x - z/2$ and

$$\Lambda^{ij}(u_0) = \dot{\Omega}^{\alpha i}(u_0)\Omega^{\alpha j}(u_0) - \dot{\Omega}^{\alpha j}(u_0)\Omega^{\alpha i}(u_0)\,. \tag{3.3}$$

We have in addition used the fact that

$$\langle R^i(u)\dot{R}^j(u)\rangle = \langle R^k(v)\dot{R}^n(v)\rangle = 0\,. \tag{3.4}$$

[7] It should be mentioned that in ref. [14] an additional approximation was used, assuming that the terms in the perturbative expansion, which are non-local in time, are exponentially suppressed. In fact, this approximation is conceptually related to the threshold expansion used in the present paper. As we shall show, however, the suppression is only power-like and will show up in subsequent orders.

JHEP02(2025)092

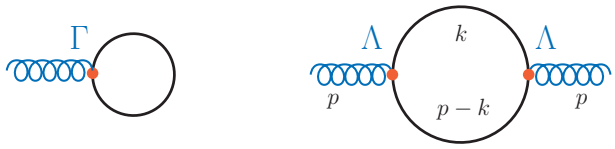

Figure 1. One-loop contributions to the self-energy: a) the tadpole diagram, b) the second-order (self-energy) diagram. The solid and wiggle lines denote the fast and the slow modes, respectively. The vertices Γ and Λ emerge from the Lagrangian (2.30) after integrating out the fast mode perturbatively, see eqs. (3.3) and (3.12).

Next, note that

$$\langle R^i(u)R^k(v)\rangle\langle\dot{R}^j(u)\dot{R}^n(v)\rangle = \frac{\delta^{ik}}{F^2}\,\frac{\delta^{nj}}{F^2}\,I_1\,,$$
$$I_1 = \int\frac{dk_0}{2\pi}\,\frac{1}{L^3}\sum_{\boldsymbol{k}\neq 0}\int\frac{dp_0}{2\pi}\,\frac{1}{L^3}\sum_{\boldsymbol{p}\neq\boldsymbol{k}}\frac{k_0^2 e^{-ipz}}{k^2(p-k)^2}\,, \tag{3.5}$$

and

$$\langle R^i(u)\dot{R}^n(v)\rangle\langle\dot{R}^j(u)R^k(v)\rangle = \frac{\delta^{\mathrm{in}}}{F^2}\,\frac{\delta^{kj}}{F^2}\,I_2\,,$$
$$I_2 = \int\frac{dk_0}{2\pi}\,\frac{1}{L^3}\sum_{\boldsymbol{k}\neq 0}\int\frac{dp_0}{2\pi}\,\frac{1}{L^3}\sum_{\boldsymbol{p}\neq\boldsymbol{k}}\frac{k_0(p_0-k_0)e^{-ipz}}{k^2(p-k)^2}\,. \tag{3.6}$$

The effective Lagrangian $\delta\mathscr{L}^{(b)}_{\mathsf{eff}}$ is essentially non-local. Consider now the loop integrals in eqs. (3.5) and (3.6). First, since the matrices $\Lambda^{ij}, \Lambda^{ik}$ in eq. (3.2) do not depend on the argument $\boldsymbol{z}$, the integration over this variable can be carried out and one gets:

$$\int d^3\boldsymbol{z}\, I_1 = \int\frac{dk_0}{2\pi}\,\frac{1}{L^3}\sum_{\boldsymbol{k}\neq 0}\int\frac{dp_0}{2\pi}\,\frac{1}{L^3}\sum_{\boldsymbol{p}\neq\boldsymbol{k}}L^3\delta_{\boldsymbol{p}0}\frac{k_0^2 e^{-ip_0z_0}}{k^2(p-k)^2}$$
$$= \int\frac{dp_0}{2\pi}\,e^{-ip_0z_0}\int\frac{dk_0}{2\pi}\,\frac{1}{L^3}\sum_{\boldsymbol{k}\neq 0}\frac{k_0^2}{k^2((p_0-k_0)^2+\boldsymbol{k}^2)}\,. \tag{3.7}$$

It is now seen that the above integral features different momentum scales. Namely, the energy of the slow mode, p_0, scales like L^{-3}, whereas the three-momentum of the fast mode, $\boldsymbol{k}$, scales like L^{-1}. It is easy to ensure that the only non-vanishing contribution to this integral comes from the region where k_0 also scales like L^{-1}. Applying the so-called threshold expansion [37] to this integral, one finally gets

$$\int d^3\boldsymbol{z}\, I_1 = \int\frac{dp_0}{2\pi}\,e^{-ip_0z_0}\int\frac{dk_0}{2\pi}\,\frac{1}{L^3}\sum_{\boldsymbol{k}\neq 0}\frac{k_0^2}{k^2(k_0^2+\boldsymbol{k}^2)}\left(1+\frac{2p_0k_0}{k_0^2+\boldsymbol{k}^2}+\cdots\right)$$
$$= \delta(z_0)\int\frac{dk_0}{2\pi}\,\frac{1}{L^3}\sum_{\boldsymbol{k}\neq 0}\frac{k_0^2}{(k^2)^2}+\cdots$$
$$= \frac{1}{4}\,\delta(z_0)\frac{1}{L^3}\sum_{\boldsymbol{k}\neq 0}\frac{1}{|\boldsymbol{k}|}+\cdots = \frac{1}{2}\,\delta(z_0)d(0)+\cdots \tag{3.8}$$

JHEP02(2025)092

The integral I_2 can be expanded similarly

$$\int d^3\boldsymbol{z}\, I_2 = -\frac{1}{2}\,\delta(z_0)d(0) + \cdots \tag{3.9}$$

Substituting this result in eq. (3.2), one obtains

$$\begin{aligned}
\delta\mathscr{L}^{(b)}_{\text{eff}}(x) &= -\frac{1}{16}\,d(0)\Lambda^{ij}(x_0)\Lambda^{kn}(x_0)(\delta^{ik}\delta^{jn} - \delta^{\text{in}}\delta^{jk}) + \cdots \\
&= -\frac{1}{4}\,d(0)(\dot\Omega^{\alpha i}(x_0)\Omega^{\alpha j}(x_0) - \dot\Omega^{\alpha j}(x_0)\Omega^{\alpha i}(x_0))\dot\Omega^{\beta i}(x_0)\Omega^{\beta j}(x_0) + \cdots \\
&= -\frac{1}{2}\,d(0)\dot\Omega^{\alpha i}(x_0)\Omega^{\alpha j}(x_0)\dot\Omega^{\beta i}(x_0)\Omega^{\beta j}(x_0) + \cdots \\
&= -\frac{1}{2}\,d(0)(\dot\Omega^{\alpha i}(x_0)\dot\Omega^{\alpha i}(x_0) - \dot\Omega^{\alpha 0}(x_0)\dot\Omega^{\alpha 0}(x_0)) + \cdots
\end{aligned} \tag{3.10}$$

This expression should be added to the tadpole contribution coming from the diagram in figure 1a. The corresponding effective Lagrangian is local and is given by

$$\begin{aligned}
\delta\mathscr{L}^{(a)}_{\text{eff}}(x) &= \frac{F^2}{2}\,\Gamma^{ij}(x_0)\langle R^i(x)R^j(x)\rangle \\
&= -\frac{N-1}{2}\,d(0)\dot e^\alpha(x_0)\dot e^\alpha(x_0) + \frac{1}{2}\,d(0)\dot\Omega^{\alpha i}(x_0)\dot\Omega^{\alpha i}(x_0)\,,
\end{aligned} \tag{3.11}$$

where

$$\Gamma^{ij}(x_0) = -\dot e^\alpha(x_0)\dot e^\alpha(x_0) + \dot\Omega^{\alpha i}(x_0)\dot\Omega^{\alpha j}(x_0)\,. \tag{3.12}$$

Hence,

$$\delta\mathscr{L}^{(a)}_{\text{eff}}(x) + \delta\mathscr{L}^{(b)}_{\text{eff}}(x) = -\frac{N-2}{2}\,d(0)\dot e^\alpha(x_0)\dot e^\alpha(x_0)\,, \tag{3.13}$$

and the result given in eq. (2.36) is readily reproduced. Hence, as expected, the physical result does not depend on the field parameterization.[8] In other words, the field transformation, introduced in refs. [13, 14, 22], ensures the separation of the fast and slow modes at the order one is working.

3.2 NNLO

The interaction Lagrangian that will be used in the calculations at NNLO is obtained by the expansion of the Lagrangian given in eqs. (2.1)–(2.3) in powers of the field $\boldsymbol{R}$. Up to the NNLO, the relevant terms are given by

$$\begin{aligned}
\mathscr{L}^{(4)} = &\frac{F^2}{2}\,\Gamma^{ij}R^iR^j + \frac{F^2}{2}\,\Lambda^{ij}R^i\dot R^j - F^3\Delta^i\boldsymbol{R}^2\dot R^i + \mathscr{L}_R \\
&- 4\ell_1 b_1^{ij}\dot R^i\dot R^j - 2\ell_2 b_2^{ij}\dot R^i\dot R^j + \cdots\,,
\end{aligned} \tag{3.14}$$

[8] Note that the final result contains only $\Omega^{\alpha 0}(t)$ and thus does not depend on the matrix Σ in eq. (2.32).

JHEP02(2025)092

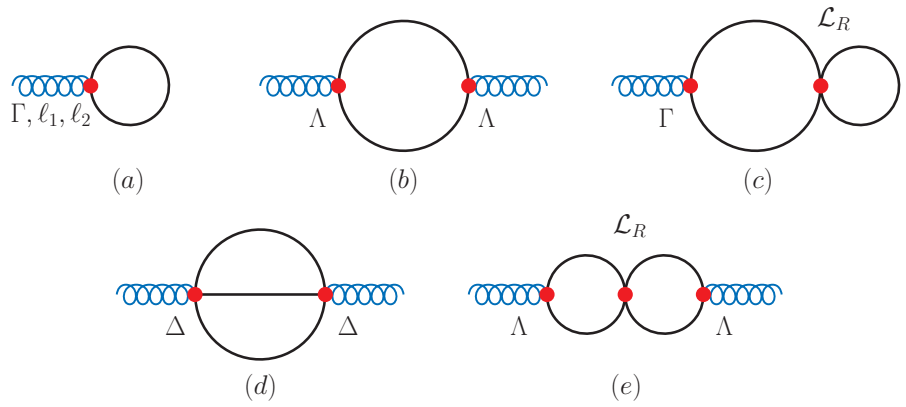

Figure 2. The diagrams contributing to the self-energy at NNLO. For notations, see figure 1.

where

$$\begin{aligned}
\Gamma^{ij} &= -\delta^{ij}\dot{e}^\alpha\dot{e}^\alpha + \dot{\Omega}^{\alpha i}\dot{\Omega}^{\alpha j}\,,\\
\Lambda^{ij} &= \dot{\Omega}^{\alpha i}\Omega^{\alpha j} - \dot{\Omega}^{\alpha j}\Omega^{\alpha i}\,,\\
\Delta^{i} &= \dot{\Omega}^{\alpha 0}\Omega^{\alpha i} - \dot{\Omega}^{\alpha i}\Omega^{\alpha 0}\,,\\
b_1^{ij} &= \dot{\Omega}^{\alpha 0}\Omega^{\alpha i}\dot{\Omega}^{\beta 0}\Omega^{\beta j}\,,\\
b_2^{ij} &= \dot{\Omega}^{\alpha 0}\dot{\Omega}^{\alpha 0}\Omega^{\beta i}\Omega^{\beta j} + \dot{\Omega}^{\alpha 0}\dot{\Omega}^{\beta 0}\Omega^{\alpha i}\Omega^{\beta j}\,,\\
\mathscr{L}_R &= (\boldsymbol{R}\partial_\mu\boldsymbol{R})^2\,.
\end{aligned} \tag{3.15}$$

Note that Γ^{ij} and Λ^{ij} have been introduced earlier, in eqs. (3.12) and (3.3), respectively. In the calculations at the NLO, only the first two terms of eq. (3.14) contribute.

Since we shall again focus on the calculation of the excitation spectrum in the rest-frame, the same shortcut as at the NLO can be used as a substitute for the general method described in section 2.1. Only the diagrams depicted in figure 2 contribute. The calculations based on the threshold expansion are pretty standard and will not be described in much detail.

Figure 2a, $\boldsymbol{\Gamma}$ + figure 2b, $\boldsymbol{\Lambda\Lambda}$. The sum of two diagrams shown in figure 2a (with the vertex Γ) and in figure 2b has been calculated already, see eq. (3.13). The result is given by

$$\delta\mathscr{L}^{\Gamma}(x) + \delta\mathscr{L}^{\Lambda\Lambda}(x) = -\frac{N-2}{2}\,d(0)\dot{e}^\alpha(x_0)\dot{e}^\alpha(x_0)\,. \tag{3.16}$$

Figure 2a, $\boldsymbol{\ell_1 + \ell_2}$. Another two contributions in the diagram in figure 2a come from the terms in the Lagrangian that contain the low-energy constants ℓ_1 and ℓ_2. These contributions are again given by the tadpoles:

$$\delta\mathscr{L}^{\ell_1}(x) + \delta\mathscr{L}^{\ell_2}(x) = \frac{(4\ell_1 + 2\ell_2 N)}{F^2}\,\ddot{d}(0)\dot{e}^\alpha(x_0)\dot{e}^\alpha(x_0)\,, \tag{3.17}$$

where

$$\ddot{d}(0) = -\int\frac{dk_0}{2\pi}\,\frac{1}{L^3}\sum_{\boldsymbol{k}\neq 0}\frac{k_0^2}{k_0^2 + \boldsymbol{k}^2}\,. \tag{3.18}$$

Note that $\ddot{d}(0) = O(L^{-4})$ and hence the above contribution comes indeed at NNLO.

JHEP02(2025)092

Figure 2c, ΓR. The contribution of the two-loop the diagram shown in figure 2c is given by

$$\delta\mathscr{L}^{\Gamma R}(x) = -\frac{1}{2F^2}\int d^4y\,\Gamma^{ii}(x_0)\left(-d^2(x-y)\partial_\mu\partial_\mu d(0) + \partial_\mu d(x-y)\partial_\mu d(x-y)d(0)\right). \tag{3.19}$$

Taking into account that

$$\begin{aligned}\partial_\mu\partial_\mu d(0) &= \int\frac{dk_0}{2\pi}\frac{1}{L^3}\sum_{\boldsymbol{k}\neq 0}\frac{-k^2}{k^2} = 0\,,\\ \int d^4y\,\partial_\mu d(x-y)\partial_\mu d(x-y) &= \int\frac{dk_0}{2\pi}\frac{1}{L^3}\sum_{\boldsymbol{k}\neq 0}\frac{k^2}{(k^2)^2} = d(0)\,,\end{aligned} \tag{3.20}$$

we finally get

$$\delta\mathscr{L}^{\Gamma R}(x) = -\frac{1}{2F^2}\,d^2(0)\left(-(N-1)\dot{e}^\alpha(x_0)\dot{e}^\alpha(x_0) + \dot{\Omega}^{\alpha i}(x_0)\Omega^{\alpha i}(x_0)\right). \tag{3.21}$$

Figure 2d, $\Delta\Delta$. The contribution of the diagram shown in figure 2d is given by

$$\delta\mathscr{L}^{\Delta\Delta}(x) = \frac{N-2}{4F^2}\int d^4y\Delta^i(x_0)\Delta^i(y_0)d^2(x-y)\ddot{d}(x-y)\,. \tag{3.22}$$

The integral above contains different scales, so the threshold expansion in p_0 is necessary:

$$\begin{aligned}&\int d^3\boldsymbol{y}d^2(x-y)\ddot{d}(x-y)\\ &= \int d^3\boldsymbol{y}\int\frac{dk_{10}dk_{20}dk_{30}}{(2\pi)^3}\frac{1}{L^9}\sum_{\boldsymbol{k}_1,\boldsymbol{k}_2,\boldsymbol{k}_3\neq 0}\frac{-k_{30}^2e^{i(k_{10}+k_{20}+k_{30})(x_0-y_0)+i(\boldsymbol{k}_1+\boldsymbol{k}_2+\boldsymbol{k}_3)(\boldsymbol{x}-\boldsymbol{y})}}{k_1^2k_2^2k_3^2}\\ &= \int\frac{dk_{10}dk_{20}dp_0}{(2\pi)^3}\frac{1}{L^6}\sum_{\boldsymbol{k}_1,\boldsymbol{k}_2,\boldsymbol{k}_3\neq 0}\frac{-\delta^3_{\boldsymbol{k}_1+\boldsymbol{k}_2+\boldsymbol{k}_3,0}(p_0-k_{10}-k_{20})^2e^{ip_0(x_0-y_0)}}{k_1^2k_2^2((p_0-k_{10}-k_{20})^2+(\boldsymbol{k}_1+\boldsymbol{k}_2)^2)}\\ &= \delta(x_0-y_0)\int\frac{dk_{10}dk_{20}}{(2\pi)^2}\frac{1}{L^6}\sum_{\boldsymbol{k}_1,\boldsymbol{k}_2\neq 0}\frac{-\left(1-\delta^3_{\boldsymbol{k}_1+\boldsymbol{k}_2,0}\right)(k_{10}+k_{20})^2}{k_1^2k_2^2((k_{10}+k_{20})^2+(\boldsymbol{k}_1+\boldsymbol{k}_2)^2)}+\cdots\end{aligned} \tag{3.23}$$

Carrying out the summation over the index i, we finally obtain

$$\delta\mathscr{L}^{\Delta\Delta}(x) = \frac{N-2}{F^2}\,e^\alpha(x_0)e^\alpha(x_0)\int d^4yd^2(y)\ddot{d}(y)+\cdots \tag{3.24}$$

Figure 2e, $\Lambda R\Lambda$. Finally, the contribution from the diagram figure 2e can be written as

$$\delta\mathscr{L}^{\Lambda R\Lambda}(x) = \frac{2}{F^2}\left(\delta^{im}\delta^{jl}-\delta^{il}\delta^{jm}\right)\int dy_0\Lambda^{ij}(x_0)\Lambda^{lm}(y_0)K(x_0,y_0)\,, \tag{3.25}$$

where

$$\begin{aligned}K(x_0,y_0) &= \int dz_0\int\frac{dp_0dq_0dk_0dl_0}{(2\pi)^4}\frac{1}{L^6}\sum_{\boldsymbol{k}_1,\boldsymbol{k}_2,\boldsymbol{l}_1,\boldsymbol{l}_2\neq 0}\delta^3_{\boldsymbol{k}_1+\boldsymbol{k}_2,0}\delta^3_{\boldsymbol{l}_1+\boldsymbol{l}_2,0}\\ &\quad\times\frac{l_0l_\mu k_0k_\mu e^{ip_0(x_0-z_0)+iq_0(z_0-y_0)}}{((p_0-l_0)^2+\boldsymbol{l}_1^2)(l_0^2+\boldsymbol{l}_1^2)((q_0-k_0)^2+\boldsymbol{k}_1^2)(k_0^2+\boldsymbol{k}_1^2)}\\ &= \frac{1}{4}\,\delta(x_0-y_0)d^2(0)+\cdots\end{aligned} \tag{3.26}$$

Again, we have used threshold expansion in p_0 and q_0 to arrive at this result. Carrying out the summation over indices i, j, l, m, we finally get

$$\delta\mathscr{L}^{\Lambda R\Lambda}(x) = \frac{1}{2F^2}\, d^2(0)\left(\dot{\Omega}^{\alpha i}(x_0)\dot{\Omega}^{\alpha i}(x_0) - \dot{e}^{\alpha}(x_0)\dot{e}^{\alpha}(x_0)\right) . \tag{3.27}$$

As at the NLO, even if the set of the diagrams differs from the ones considered in ref. [14], one arrives exactly at the same result after adding all contributions and canceling terms with $\dot{\Omega}^{\alpha i}\dot{\Omega}^{\alpha i}$. Namely, the expression for the correction to the moment of inertia at this order takes the form

$$\Theta = F^2 L^3\left(1 + \frac{C_1}{(FL)^2} + \frac{C_2}{(FL)^4} + \frac{C_3}{(FL)^4}\,\ln(FL)\right) , \tag{3.28}$$

where C_1, C_2, C_3, expressed in terms of the loop integrals, are exactly the same as in ref. [14]. This result was of course expected, since observables should not depend on the choice of the interpolating field.[9] In addition, it becomes clear that, contrary to the claim of ref. [14], the subleading terms in the threshold expansion are only power-law suppressed and not exponentially suppressed.

It should be also mentioned that an alternative calculation of the mass gap to this order exists [40], which does not coincide with the result of ref. [14]. Unfortunately, no details of calculation are given in ref. [40], so it is impossible to track the reason for this difference unambiguously. In particular, the final expression for the mass gap differs from our expression at two places, that affects the value of the coefficient C_2. First, the eq. (5.20) in ref. [40] contains an additional term proportional to the quantity $\beta_1^{(3)}$. This term should stem from the zero mode contribution to the effective action, see eq. (3.7) of ref. [40]. This contribution is absent in ref. [14] as well as in the present paper, because it is proportional to $\delta(0)$ that vanishes in the split dimensional regularization (for the origin of this factor, see, e.g., ref. [41]). The second difference emerges in the calculation of the loop integral in eq. (3.24) of the present paper, see eqs. (5.17)-(5.18) of ref. [40] and the discussion that follows (more details are given in ref. [42]). We opt not to comment on this difference before carrying out all calculations of the loop diagrams ourselves. This, question, however, has not been the main aim of the present paper that is focused on restoring the power counting with the use of the threshold expansion, and is relegated to our future publications.

The generalization of the approach to any order is crystal-clear. Evaluating arbitrary Green functions, one first has to integrate out the fast modes corresponding to the field $\boldsymbol{R}(x)$. Then, one obtains multi-scale Feynman integrals whose counting in the small parameter $1/L$ is obscure. The key observation is that the power counting can be formulated by performing the threshold expansion in all integrals. After that, calculations can proceed without further ado. The vacuum matrix elements of the product of the fields $\Omega^{\alpha\beta}(t)$ and derivatives thereof can be then calculated along the lines described in appendix B. Stated differently, the fast and slow modes are integrated out separately and the result is "glued together" in order to arrive at the final expression for the Green functions. Furthermore, as argued in appendix D, the large momenta (of order of L^{-1}) do not appear in the matrix elements with the slow modes and thus threshold expansion is not necessary there.

[9] Furthermore, the logarithm in eq. (3.28) emerges from the two-loop diagram in figure 2d, see eq. (3.24). Details of calculations are given in ref. [14].

JHEP02(2025)092

Finally, we make a short remark concerning renormalization. Potentially, ultraviolet divergences may arise at two different places: in the Feynman diagrams with the fast modes, and in the infinite sums that are present in the Green functions of the slow modes. Consider first the fast modes. The Feynman integrals emerging here are identical to the ordinary ones, with the $\boldsymbol{k} = 0$ component removed. This removal, however, does not affect the ultraviolet divergences. On the other hand, as argued in appendix B, all matrix elements containing slow modes are ultraviolet-finite. Hence, as expected, the couplings that are present in the effective Lagrangian suffice to remove all ultraviolet divergences, and the pertinent β functions coincide with the ones in the infinite volume.

4 Conclusion and outlook

Effective field theory methods allow one to study the temperature and volume dependence of QCD, as well as different condensed-matter models, whose behavior in the long-wavelength limit can be described by effective chiral Lagrangians. According to the particular values of the parameters T and L, as well as the lowest mass in the system (the pion mass, M), the perturbative expansion of the physical observables in these parameters should be rearranged, corresponding to what is termed as different regimes.

The perturbative expansion of the effective theory in the δ regime, unlike the p- and ϵ-regimes, is characterized by the presence of two distinct energy scales, corresponding to the so-called slow and fast pions. Such a separation is unnecessary in the p-regime, whereas in the ϵ-regime the slow mode is not a dynamical variable. Only in the δ-regime, in which the time-dependent slow mode emerges, one is faced with the above-mentioned problem. For this reason, the perturbative calculations, up to now, have been limited to the lower orders in the expansion, and some cleverly designed tricks (like the field transformation considered in the present paper) were used to restore power counting at higher orders.

The key observation made in the present paper was that the application of the threshold expansion to the Feynman integrals appearing in the perturbative expansion allows one to address the problem simultaneously at all orders and to rectify the power counting without resorting to further tricks. The known results for the rest-frame excitation spectrum at NNLO have been readily reproduced in a straightforward manner, demonstrating the independence of the physical observables on the choice of the interpolating field. The proposed method, on one hand, paves way for a systematic calculation of other observables in QCD and condensed matter physics even at higher orders and, on the other hand, can be generalized to the case, when the massive fermions interacting with pions, are present (this Lagrangian describes the physics of hole-doped antiferromagnets in the long-wavelength limit). In addition, an intriguing question arises, whether it is possible to implement the threshold expansion at the Lagrangian level using so-called labeled fields (like in case of the heavy quark effective theory of QCD) that would render power counting explicit. These issues form the subject of future investigations.

JHEP02(2025)092

Acknowledgments

The authors thank Thomas Becher, Jürg Gasser, George Jackeli, Heinrich Leutwyler, Tom Luu, Johann Ostmeyer and Uwe Wiese for interesting discussions. We would like to especially thank Martin Beneke for critical reading of the manuscript and numerous suggestions that helped to improve the original draft considerably. The work of was funded in part by the Deutsche Forschungsgemeinschaft (DFG, German Research Foundation) — Project-ID 196253076 — TRR 110. AR acknowledges the financial support from the Ministry of Culture and Science of North Rhine-Westphalia through the NRW-FAIR project and from the Chinese Academy of Sciences (CAS) President's International Fellowship Initiative (PIFI) (grant no. 2024VMB0001). The work of UGM was also supported by the CAS President's International Fellowship Initiative (PIFI) (Grant No. 2025PD00NN).

A Wick's theorem for the slow modes?

As already mentioned, Wick's theorem cannot be used if the free Lagrangian describes the rigid rotator rather than a harmonic oscillator. We shall demonstrate this (rather obvious) statement here in an explicit example in the $O(3)$ model. Here, the eigenstates coincide with the eigenvectors of the angular momenta $|n\rangle = |\ell m\rangle$, and the eigenvalues are given by the expression $\varepsilon_\ell = \ell(\ell+1)/\Theta$. To simplify things as much as possible, we consider the Green functions of the fields $e^0(t)$. Then,

$$\begin{aligned}\langle \ell' m'|e^0|\ell m\rangle &= \int d\Omega Y^*_{\ell' m'}(\Omega)\sqrt{\frac{4\pi}{3}}Y_{10}(\Omega)Y_{\ell m}(\Omega)\\ &= \sqrt{(2\ell'+1)(2\ell+1)}(-1)^{m'}\begin{pmatrix}1 & \ell & \ell'\\ 0 & m & -m'\end{pmatrix}\begin{pmatrix}1 & \ell & \ell'\\ 0 & 0 & 0\end{pmatrix}. \end{aligned} \tag{A.1}$$

In the calculation of the Green functions of the field $e^0(t)$, we can set $m = m' = 0$. Using explicit values of the Wigner $3-j$ symbols, one gets

$$\begin{aligned}\langle 0,0|e^0|1,0\rangle &= \langle 1,0|e^0|0,0\rangle = \frac{1}{\sqrt{3}},\\ \langle 1,0|e^0|2,0\rangle &= \langle 2,0|e^0|1,0\rangle = \frac{2}{\sqrt{15}}. \end{aligned} \tag{A.2}$$

With the use of the above formula, the two-point and the four-point functions of the field $e^0(t)$ can be written as follows

$$\begin{aligned}\langle e^0(t_1)e^0(t_2)\rangle &= \frac{1}{3}\left(e^{-(\varepsilon_1-\varepsilon_0)(t_1-t_2)}\theta(t_1-t_2) + e^{-(\varepsilon_1-\varepsilon_0)(t_2-t_1)}\theta(t_2-t_1)\right)\\ &= \frac{1}{3}\exp\left(-\frac{|t_1-t_2|}{\Theta}\right), \end{aligned} \tag{A.3}$$

and

$$\begin{aligned}\langle e^0(t_1)e^0(t_2)e^0(t_3)e^0(t_4)\rangle = &\sum_{\text{perm } ijkl}\theta(t_i-t_j)\theta(t_j-t_k)\theta(t_k-t_l)\\ &\times\left[\frac{1}{9}\exp\left(-\frac{t_i-t_j+t_k-t_l}{\Theta}\right)+\frac{16}{225}\exp\left(-\frac{t_i+2t_j-2t_k-t_l}{\Theta}\right)\right], \end{aligned} \tag{A.4}$$

JHEP02(2025)092

where perm $ijkl$ denotes all possible permutations of the indices. It can be explicitly verified that the Wick's theorem does not hold. On the other hand, considering the case of the harmonic oscillator, one may construct a similar four-point function

$$\begin{aligned}\langle a(t_1)a(t_2)a^\dagger(t_3)a^\dagger(t_4)\rangle &= e^{-\omega(t_1+t_2-t_3-t_4)} \\ &\times\Bigg[2\sum_{ijkl=1234,2134,1243,2143}\theta(t_i-t_j)\theta(t_j-t_k)\theta(t_k-t_l) \\ &\quad+\sum_{ijkl=1324,2314,1423,2413}\theta(t_i-t_j)\theta(t_j-t_k)\theta(t_k-t_l)\Bigg] \\ &= e^{-\omega(t_1+t_2-t_3-t_4)}\Big[\theta(t_1-t_3)\theta(t_2-t_4)+\theta(t_1-t_4)\theta(t_2-t_3)\Big]\,. \end{aligned} \tag{A.5}$$

Here, ω denotes the energy of a single excitation, and the matrix elements of the creation/annihilation operators are normalized in the following way

$$\langle 0|a|1\rangle = \langle 1|a^\dagger|0\rangle = 1\,, \qquad \langle 1|a|2\rangle = \langle 2|a^\dagger|1\rangle = \sqrt{2}\,. \tag{A.6}$$

It is immediately seen that the Wick's theorem holds in the case of an oscillator.

To summarize, one sees that the validity of the Wick's theorem is tied to the choice of the free Lagrangian. In our context, it is important to realize that, for this reason, it is impossible to single out the contribution of slow modes at the level of individual Feynman integrals, using, e.g., some kind of the threshold expansion, because slow modes are inherently non-perturbative.

B Calculation of the matrix elements with the slow modes

As we have seen, the path integral over the slow modes cannot be calculated by using the standard diagrammatic technique. The reason for this is that the unperturbed part of the Lagrangian of the slow modes coincides with the Lagrangian of the rigid rotator rather than that of an harmonic oscillator. As noted above, in order to evaluate the vacuum expectation value of the operators containing slow modes, one may insert a full set of the eigenvectors of the unperturbed Hamiltonian between each two operators. Consider, for example, the Green function

$$\begin{aligned}G(t_1,\cdots,t_m) = \prod_t\int d^N e(t)\delta(e^\alpha e^\alpha-1)\exp\Big(-\frac{\Theta}{2}\int dt\,\dot e^\alpha(t)\dot e^\alpha(t)\Big) \\ \times O_1\left[e(t_1)\right]\cdots O_m\left[e(t_m)\right]\,,\end{aligned} \tag{B.1}$$

where $O_1,\ldots,O_m$ are arbitrary local operators built of $e^\alpha(t)$ (and time derivatives thereof which enter polynomially in the expression). Assume, for instance that $t_1>t_2>\ldots>t_m$. Then, the above Green function can be represented by a sum

$$\begin{aligned}G(t_1,\cdots,t_m) = \sum_{n_1,\ldots,n_{m-1}} e^{-\varepsilon_{n_1}(t_1-t_2)-\cdots-\varepsilon_{n_{m-1}}(t_{m-1}-t_m)} \\ \times\langle 0|O_1|n_1\rangle\cdots\langle n_{m-1}|O_m|0\rangle\,.\end{aligned} \tag{B.2}$$

JHEP02(2025)092

In case of the $O(N)$ rigid rotator, the eigenfunctions of the Laplace operator are given by pertinent hyperspherical harmonics (see, e.g., [43]). The polar coordinates are introduced as

$$\begin{aligned} e^0 &= \cos\theta_1\,, \\ e^1 &= \sin\theta_1 \cos\theta_2\,, \\ e^2 &= \sin\theta_1 \sin\theta_2 \cos\theta_3\,, \\ &\cdots \\ e^{N-2} &= \sin\theta_1 \cdots \sin\theta_{N-2} \cos\varphi\,, \\ e^{N-1} &= \sin\theta_1 \cdots \sin\theta_{N-2} \sin\varphi\,, \end{aligned} \tag{B.3}$$

and the hyperspherical harmonics are given by

$$Y(m_k;\theta_k,\pm\varphi) = N^{-1/2}(m_k) e^{\pm i m_{N-2}\varphi} \prod_{k=0}^{N-3} C_{m_k-m_{k+1}}^{m_{k+1}+\frac{N-1-k}{2}}(\cos\theta_{k+1})\,. \tag{B.4}$$

Here, the m_k are the integers

$$n = m_0 \geq m_1 \geq \cdots m_{N-2} \geq 0\,, \tag{B.5}$$

where the index n labels the irreducible representations (an analog of the angular momentum ℓ in case of the $O(3)$ group).[10] Furthermore, the $C_n^\mu(x)$ denote Gegenbauer polynomials

$$C_n^\mu(x) = \frac{\Gamma(n+2\mu)}{\Gamma(n+1)\Gamma(2\mu)}\ {}_2F_1\left(-n, n+2\mu, \mu+\frac{1}{2}, \frac{1}{2}-\frac{1}{2}\,x\right)\,. \tag{B.6}$$

The normalization constant is given by

$$\begin{aligned} N(m_0,\cdots m_{N-2}) &= 2\pi \prod_{k=1}^{N-2} E_k(m_{k-1},m_k)\,, \\ E_k(l,m) &= \pi \frac{2^{k-2m-N+2}\Gamma(l+m+N-1-k)}{\left(l+\frac{N-1-k}{2}\right)(l-m)!\left(\Gamma\left(m+\frac{N-1-k}{2}\right)\right)^2}\,. \end{aligned} \tag{B.7}$$

The eigenvalues ε_n are given by eq. (2.29).

Assume first that the operator $O(e)$ does not contain time derivatives of e^α. Then, the matrix element of such an operator between two eigenstates characterized by the sets $n \doteq \{m_k\}$ and $n' \doteq \{m'_k\}$ with $k = 0,\ldots,N-2$ is given by

$$\langle n|O|n'\rangle = \int d\Omega_N Y^*(m_k;\theta_k,\pm\varphi) O\left[e(\theta_k,\varphi)\right] Y(m'_k;\theta_k,\pm\varphi)\,, \tag{B.8}$$

where $d\Omega_N$ denotes the volume in the N-dimensional space

$$d\Omega_N = (\sin\theta_1)^{N-2} \cdots \sin\theta_{N-2} d\theta_1 \cdots d\theta_{d-2} d\varphi\,. \tag{B.9}$$

In case when the operator $O\,[e]$ has a polynomial dependence on e^α, the matrix elements $\langle n|O|n'\rangle$ are nonvanishing for selected values on n, n', owing to the Wigner-Eckart theorem.

[10] The need for both signs $\pm$ in eq. (B.4) is related to our convention $m_{N-2} \geq 0$.

JHEP02(2025)092

Note however that, for example, the operator Ω^{ij} is not a polynomial in e^α. On the contrary, the dependence on time derivatives always has a polynomial form. Consider, for instance, the operator $O = \tilde{O}\,[e]\,\dot{e}^\alpha$, where the operator $\tilde{O}$ does not contain time derivatives. The matrix element of this operator is given by

$$\langle n|O|n'\rangle = \sum_{n''}\langle n|\tilde{O}|n''\rangle(\varepsilon_{n'} - \varepsilon_{n''})\langle n''|e^\alpha|n'\rangle\,. \tag{B.10}$$

The matrix element $\langle n''|e^\alpha|n'\rangle$ obeys selection rules in n', n'' and α (Wigner-Eckart theorem).[11] Hence, the summation over n'' can be carried out explicitly.

To summarize, if all operators present in (B.1) are polynomials in e^α, all sums over intermediate states can be carried out in a closed form and contain only a finite number of terms. From this it immediately follows that there are no (ultraviolet) divergences in this case. Hence, the Green functions of $\Omega^{\alpha\beta}(t)$ with $\alpha = 0$ and/or $\beta = 0$ are ultraviolet-finite, as well as time derivatives thereof to all orders. In case of a non-polynomial dependence, as in $\Omega^{ij}(t)$, (infinite) sums remain in a final expression. These sums are anyway convergent for $t_1 \neq t_2 \neq \cdots \neq t_m$, due to the presence of the exponential damping factors. This argument does not apply, however, if any two (or more) arguments coincide. Thus, the (potential) divergences in the position space must be proportional to $\delta(t_i - t_j)$ and derivatives thereof and can therefore be removed by local counterterms in the effective Lagrangian that contain slow degrees of freedom only. It is straightforward to see, however, that there is no need for such counterterms at all. Indeed, consider first the case when no time derivatives are present. The matrix elements of $\Omega^{ij}(t)$ itself are finite, since $e^i e^j/(1+e^0)$ is a regular function even at $e^0 \to -1$. Furthermore, at coinciding time arguments we merely get a product of two (or more) operators $\Omega^{ij}(t)\Omega^{kn}(t)\ldots$, whose matrix elements are also finite. Further, the derivative terms always contain the quantity $\dot{e}^\alpha(t)$ polynomially and thus do not lead to the divergences as well. Finally, since the Lagrangian is built only of $\Omega^{\alpha\beta}$ and time derivatives thereof, we come to the conclusion that all Green functions of the fields $\Omega^{\alpha\beta}(t)$ and their time derivatives are ultraviolet-finite.

C Field transformation

Below, we consider the field transformation introduced in refs. [13, 14, 22], in its continuum version. In order to specify the matrix $\Sigma(t)$ in eq. (2.33), we first define the matrix $V(t', t) \in O(N)$ that obeys the first-order differential equation

$$\frac{\partial}{\partial t}\,V(t', t) = \Sigma(t')\Omega^T(t')\frac{\partial}{\partial t}\,\Omega(t)\,. \tag{C.1}$$

The following boundary condition is imposed

$$V(t, t) = \Sigma(t)\,, \tag{C.2}$$

where $\Sigma(t')$ is the matrix defined in eq. (2.33), and

$$\hat{\Sigma}^{ij}(t) = V^{ij}(t', t) - \frac{V^{i0}(t', t)V^{0j}(t', t)}{1 + V^{00}(t', t)}\,. \tag{C.3}$$

[11] For example, in case of the $O(3)$ group, the eigenstates are labeled as $|n\rangle \doteq |\ell m\rangle$, and the matrix element $\langle \ell'' m''|r^m|\ell' m'\rangle$ is non-zero, if and only if $\ell'' = \ell' \pm 1$ and $m'' = m + m'$.

JHEP02(2025)092

These equations determine $\Sigma(t)$ any given time t, provided its initial value is fixed. Note that the argument t' in $\Sigma(t)$ is implicit (we remind the reader that the boundary conditions are set at $t = t'$).

Let us now differentiate both sides of eq. (C.3) with respect to the variable t and consider the limit $t' \to t$ afterwards. The differentiation gives

$$\begin{aligned}\frac{\partial}{\partial t}\hat{\Sigma}^{ij}(t) = \frac{\partial}{\partial t}V^{ij}(t',t) - \frac{V^{0j}(t',t)}{1+V^{00}(t',t)}\frac{\partial}{\partial t}V^{i0}(t',t) \\ - \frac{V^{i0}(t',t)}{1+V^{00}(t',t)}\frac{\partial}{\partial t}V^{0j}(t',t) + \frac{V^{i0}(t',t)V^{0j}(t',t)}{(1+V^{00}(t',t))^2}\frac{\partial}{\partial t}V^{00}(t',t)\,.\end{aligned} \tag{C.4}$$

On the other hand, from the boundary condition in eq. (C.1) we get that $V^{i0}(t,t) = V^{0j}(t,t) = 0$ and $V^{00}(t,t) = 1$. Hence,

$$\lim_{t'\to t}\frac{\partial}{\partial t}\hat{\Sigma}^{ij}(t) = \lim_{t'\to t}\frac{\partial}{\partial t}V^{ij}(t',t)\,. \tag{C.5}$$

Furthermore, the differential equation (C.1) at $t' \to t$ yields:

$$\lim_{t'\to t}\frac{\partial}{\partial t}\hat{\Sigma}^{ij}(t) = \lim_{t'\to t}\hat{\Sigma}^{ik}(t)\left(\Omega^T(t')\frac{\partial}{\partial t}\Omega(t)\right)^{kj}\,, \tag{C.6}$$

or, finally,

$$\left(\Sigma^T(t)\dot{\Sigma}(t)\right)^{ij} = \left(\Omega^T(t)\dot{\Omega}(t)\right)^{ij}\,, \tag{C.7}$$

where the limit $t' \to t$ on the left-hand side is implicit.

Next, let us consider the Lagrangian given in eq. (2.30). After the field redefinition, the quantity $\dot{\Omega}^{\alpha i}\Omega^{\alpha j}$ in the last term turns into

$$\begin{aligned}\left(\frac{d}{dt}(\Sigma\Omega^T)(\Omega\Sigma^T)\right)^{ij} &= \left((\dot{\Sigma}\Omega^T + \Sigma\dot{\Omega}^T)\Omega\Sigma^T\right)^{ij} \\ &= (\dot{\Sigma}\Sigma^T)^{ij} - \Sigma^{ik}(\Omega^T\dot{\Omega})^{km}(\Sigma^T)^{mj} = 0\,.\end{aligned} \tag{C.8}$$

The last equality follows from eq. (C.7).

Next, let us consider the term $\dot{\Omega}^{\alpha i}\dot{\Omega}^{\alpha j}$, which emerges in the same Lagrangian. Using field transformation and partial integration, it can be rewritten as

$$\frac{d}{dt}(\Omega\Sigma^T)^{\alpha i}\frac{d}{dt}(\Omega\Sigma^T)^{\alpha j} = \frac{d}{dt}\left((\Omega\Sigma^T)^{\alpha i}\frac{d}{dt}(\Omega\Sigma^T)^{\alpha j}\right) - (\Omega\Sigma^T)^{\alpha i}\frac{d^2}{dt^2}(\Omega\Sigma^T)^{\alpha j}\,. \tag{C.9}$$

We have already shown that the first term vanishes. The second term can be rewritten as

$$\begin{aligned}-\lim_{t'\to t}(\Omega(t)\Sigma^T(t))^{\alpha i}\frac{d^2}{dt'^2}(\Omega(t')\Sigma^T(t'))^{\alpha i} &= -\lim_{t'\to t}\frac{d^2}{dt'^2}(V^{ik}(t')(\Sigma^T(t'))^{kj}) \\ &= -\lim_{t'\to t}\frac{d^2}{dt'^2}\left(V^{ik}(t')\left(V^{jk}(t') - \frac{V^{j0}(t')V^{0k}(t')}{1+V^{00}(t')}\right)\right) \\ &= -\lim_{t'\to t}\frac{d^2}{dt'^2}\frac{V^{i0}(t')V^{j0}(t')}{1+V^{00}(t')}\,.\end{aligned} \tag{C.10}$$

JHEP02(2025)092

Taking now into account the boundary conditions on V^{00}, V^{i0}, V^{0j} at $t' = t$, one finally gets

$$-\lim_{t'\to t}(\Omega(t)\Sigma^T(t))^{\alpha i}\frac{d^2}{dt'^2}\left(\Omega(t')\Sigma^T(t')\right)^{\alpha i} = \frac{1}{2}\,\dot{V}^{i0}(t)\dot{V}^{j0}(t)\,. \tag{C.11}$$

On the other hand,

$$\dot{V}^{i0}(t) = \lim_{t'\to t}\frac{d}{dt'}\left(\Sigma(t)\Omega^T(t)\Omega(t')\right)^{i0} = (\Sigma(t)\Omega^T(t))^{i\alpha}\dot{e}^{\alpha}(t)\,. \tag{C.12}$$

In particular, summing up over the indices i, j we arrive at a simple result quoted in refs. [13, 14, 22]:

$$\dot{V}^{i0}(t)\dot{V}^{i0}(t) = \dot{e}^{\alpha}(t)\dot{e}^{\alpha}(t)\,, \tag{C.13}$$

from which Eq, (2.35) directly follows.

D Is there a large scale present in the matrix elements with the slow modes?

In this appendix, we shall argue that the threshold expansion carried out in the Feynman integrals solves the problem with the violation of the power counting *everywhere,* i.e., there is no need for additional measures in the matrix elements containing slow modes. We shall explain the meaning of this statement in a particular example. No attempt will be made to rigorously generalize it, albeit such a generalization seems to us to be relatively straightforward.

For definiteness, let us consider the following four-point function

$$G_4(\{p_i\}) = \int\prod_i^4 d^4x_i e^{-ip_ix_i}\langle S(x_1)S(x_2)S(x_4)S(x_4)\rangle\,. \tag{D.1}$$

Note that, in order to ease the notations, we shall discard all indices, derivative couplings, overall normalization factors, etc. For example, the operator $S(x)$ is given by a product $S(x) = \Omega(x_0)R(x)$. We shall further concentrate on a typical two-loop contribution to this Green function shown in figure 3. The interaction Lagrangian in the vertices will be chosen in a simple form $\mathscr{L}_{\mathsf{int}}(x) = R^4(x)O(x_0)$, where the operator O collects soft modes. Integrating out fast modes leads to the following expression:

$$\begin{aligned} G_4(\{p_i\}) = \int\prod_i^4 dx_{i0}e^{-ip_{i0}x_{i0}}\int du_0dv_0dz_0\langle\Omega(x_{10})\cdots\Omega(x_{40})O(u_0)O(v_0)O(z_0)\rangle \\ \times K(\{\boldsymbol{p}_i\},\{x_{i0}\};u_0,v_0,z_0)\,, \end{aligned} \tag{D.2}$$

where

$$\begin{aligned} K(\{\boldsymbol{p}_i\},\{x_{i0}\};u_0,v_0,z_0) = \int d^3\boldsymbol{x}_1\cdots d^3\boldsymbol{x}_4 e^{-i(\boldsymbol{p}_1\boldsymbol{x}_1+\cdots+\boldsymbol{p}_4\boldsymbol{x}_4)} \\ \times d(x_1-u)d^2(u-v)d(x_2-v)d(x_3-z)d(x_4-z)\,. \end{aligned} \tag{D.3}$$

JHEP02(2025)092

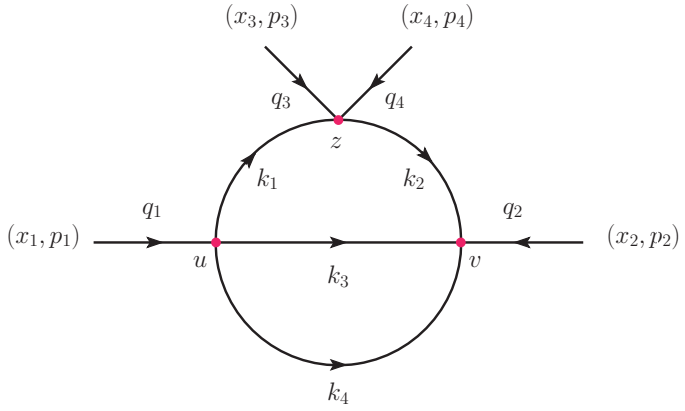

Figure 3. A typical two-loop diagram. Notations for momenta and vertices are the same as in the text.

Next, we substitute the Fourier-transform for each propagator of the fast mode (2.20). After this substitution, the argument of the exponential e^{iA} containing only zeroth components of momenta is given by[12]

$$\begin{aligned} A = {} & q_{10}x_{10} + q_{20}x_{20} + q_{30}x_{30} + q_{40}x_{40} + (-q_{10} + k_{10} + k_{30} + k_{40})u_0 \\ & + (-q_{20} - k_{20} - k_{30} - k_{40})v_0 + (-q_{30} - q_{40} - k_{10} + k_{20})z_0 \,. \end{aligned} \tag{D.4}$$

Next, we define the "small" momenta p_0, q_0, corresponding to the slow mode:

$$\begin{aligned} p_0 &= k_{10} + k_{30} + k_{40} - q_{10} \,, \\ q_0 &= -k_{20} - k_{30} - k_{40} - q_{20} \,, \\ \Delta &= q_{30} + q_{40} + k_{10} - k_{20} - p_0 - q_0 = q_{10} + q_{20} + q_{30} + q_{40} \,. \end{aligned} \tag{D.5}$$

The Feynman integral, corresponding to the two-loop diagram in Fiq. 3, is given by

$$\begin{aligned} I = {} & \int \frac{dk_{30}dk_{40}}{(2\pi)^2} \frac{1}{L^6} \sum_{\boldsymbol{k}_3, \boldsymbol{k}_4 \neq 0} \frac{1}{((p_0 + q_{10} - k_{30} - k_{40})^2 + (\boldsymbol{q}_1 - \boldsymbol{k}_3 - \boldsymbol{k}_4)^2)} \\ & \times \frac{1}{((q_0 + q_{20} + k_{30} + k_{40})^2 + (\boldsymbol{q}_2 + \boldsymbol{k}_3 + \boldsymbol{k}_4)^2)(k_{30}^2 + \boldsymbol{k}_3^2)(k_{40}^2 + \boldsymbol{k}_4^2)} \,. \end{aligned} \tag{D.6}$$

Applying threshold expansion amounts to expanding the integrand in powers of p_0, q_0. At the first order, I does not depend on these variables at all, and a subsequent integration of the exponent e^{iA} over p_0, q_0 yields δ-functions:

$$E = \exp\left(i \sum_{i=1}^{4} q_{i0}x_{i0} - iz_0\Delta \right) \delta(u_0 - z_0)\delta(v_0 - z_0) + \cdots \tag{D.7}$$

In higher orders, the derivatives of the delta functions will emerge.

At the next step, the result should be convoluted with the matrix element of the slow operators in eq. (D.2). Potential danger arises from the factor $e^{-iz_0\Delta}$, because Δ contains

[12] The momenta are defined in figure 3.

the energies of the fast modes and the convolution could inject the large momentum into the matrix element of the slow modes. It is easy to see, however, that this does not happen. Indeed, using translational invariance of the matrix element, one can shift all arguments of the operators by z_0. The dependence on z_0 in the factor E disappears and instead emerges in the exponential $\exp\left(i\sum_{i=1}^{4} p_{i0}x_{i0}\right)$, which is also present eq. (D.2). Carrying out integration over z_0 yields a trivial delta-function, corresponding to the conservation of total energy, with no hard scales present in the remainder.

As mentioned above, we make no attempt here to apply the same argument to a generic multi-loop diagram, albeit the fact that the argument is based only on the conservation of energy makes it very likely that this may work in other cases as well. Putting differently, it is known that the large momenta should be conserved separately. Here, we claim that these large momenta can be routed through the fast lines so that they are never injected in the matrix elements of the slow modes. A detailed investigation of this claim, however, forms a subject of a separate investigation, and we plan to undertake it in the future.

Data Availability Statement. This article has no associated data or the data will not be deposited.

Code Availability Statement. This article has no associated code or the code will not be deposited.

References

[1] H. Leutwyler, *Energy Levels of Light Quarks Confined to a Box*, *Phys. Lett. B* **189** (1987) 197 [INSPIRE].

[2] J. Gasser and H. Leutwyler, *Spontaneously broken symmetries: Effective lagrangians at finite volume*, *Nucl. Phys. B* **307** (1988) 763 [INSPIRE].

[3] M. Lüscher, *Two particle states on a torus and their relation to the scattering matrix*, *Nucl. Phys. B* **354** (1991) 531 [INSPIRE].

[4] M.T. Hansen and S.R. Sharpe, *Relativistic, model-independent, three-particle quantization condition*, *Phys. Rev. D* **90** (2014) 116003 [arXiv:1408.5933] [INSPIRE].

[5] M.T. Hansen and S.R. Sharpe, *Expressing the three-particle finite-volume spectrum in terms of the three-to-three scattering amplitude*, *Phys. Rev. D* **92** (2015) 114509 [arXiv:1504.04248] [INSPIRE].

[6] H.-W. Hammer, J.-Y. Pang and A. Rusetsky, *Three-particle quantization condition in a finite volume: 1. The role of the three-particle force*, *JHEP* **09** (2017) 109 [arXiv:1706.07700] [INSPIRE].

[7] H.-W. Hammer, J.-Y. Pang and A. Rusetsky, *Three particle quantization condition in a finite volume: 2. General formalism and the analysis of data*, *JHEP* **10** (2017) 115 [arXiv:1707.02176] [INSPIRE].

JHEP02(2025)092

[8] M. Mai and M. Döring, *Three-body Unitarity in the Finite Volume*, *Eur. Phys. J. A* **53** (2017) 240 [arXiv:1709.08222] [INSPIRE].

[9] J. Gasser and H. Leutwyler, *Light Quarks at Low Temperatures*, *Phys. Lett. B* **184** (1987) 83 [INSPIRE].

[10] F.C. Hansen and H. Leutwyler, *Charge correlations and topological susceptibility in QCD*, *Nucl. Phys. B* **350** (1991) 201 [INSPIRE].

[11] P. Hasenfratz and H. Leutwyler, *Goldstone Boson Related Finite Size Effects in Field Theory and Critical Phenomena With O(N) Symmetry*, *Nucl. Phys. B* **343** (1990) 241 [INSPIRE].

[12] P.F. Bedaque, H.W. Griesshammer and G. Rupak, *A nucleon in a tiny box*, *Phys. Rev. D* **71** (2005) 054015 [hep-lat/0407009] [INSPIRE].

[13] P. Hasenfratz and F. Niedermayer, *Finite size and temperature effects in the AF Heisenberg model*, *Z. Phys. B* **92** (1993) 91 [hep-lat/9212022] [INSPIRE].

[14] P. Hasenfratz, *The QCD rotator in the chiral limit*, *Nucl. Phys. B* **828** (2010) 201 [arXiv:0909.3419] [INSPIRE].

[15] M.E. Matzelle and B.C. Tiburzi, *Low-Energy QCD in the Delta Regime*, *Phys. Rev. D* **93** (2016) 034506 [arXiv:1512.05286] [INSPIRE].

[16] W. Bietenholz et al., *Pion in a Box*, *Phys. Lett. B* **687** (2010) 410 [arXiv:1002.1696] [INSPIRE].

[17] F.D.M. Haldane, *Nonlinear field theory of large spin Heisenberg antiferromagnets. Semiclassically quantized solitons of the one-dimensional easy Axis Neel state*, *Phys. Rev. Lett.* **50** (1983) 1153 [INSPIRE].

[18] F.D.M. Haldane, *Continuum dynamics of the 1-D Heisenberg antiferromagnetic identification with the O(3) nonlinear sigma model*, *Phys. Lett. A* **93** (1983) 464 [INSPIRE].

[19] S. Chakravarty, B.I. Halperin and D.R. Nelson, *Two-dimensional quantum Heisenberg antiferromagnet at low temperatures*, *Phys. Rev. B* **39** (1989) 2344 [INSPIRE].

[20] P. Hasenfratz, *Perturbation Theory and Zero Modes in $O(N)$ Lattice σ Models*, *Phys. Lett. B* **141** (1984) 385 [INSPIRE].

[21] H. Neuberger and T. Ziman, *Finite size effects in Heisenberg antiferromagnets*, *Phys. Rev. B* **39** (1989) 2608 [INSPIRE].

[22] M. Weingart, *The QCD rotator with a light quark mass*, arXiv:1006.5076 [INSPIRE].

[23] F. Niedermayer and C. Weiermann, *The rotator spectrum in the delta-regime of the O(n) effective field theory in 3 and 4 dimensions*, *Nucl. Phys. B* **842** (2011) 248 [arXiv:1006.5855] [INSPIRE].

[24] F. Niedermayer and P. Weisz, *Isospin susceptibility in the $O(n)$ sigma-model in the delta-regime*, *JHEP* **06** (2017) 150 [arXiv:1703.10564] [INSPIRE].

[25] J. Balog, F. Niedermayer and P. Weisz, *On the rotator Hamiltonian for the $SU(N) \times SU(N)$ sigma-model in the delta-regime*, *PTEP* **2020** (2020) 073B04 [arXiv:1912.05232] [INSPIRE].

[26] F. Niedermayer and P. Weisz, *Casimir squared correction to the standard rotator Hamiltonian for the $O(n)$ sigma-model in the delta-regime*, *JHEP* **05** (2018) 070 [arXiv:1801.06858] [INSPIRE].

[27] C.P. Hofmann, *Ferromagnets and antiferromagnets in the effective Lagrangian perspective*, *AIP Conf. Proc.* **623** (2002) 305 [cond-mat/0202153] [INSPIRE].

[28] C.P. Hofmann, *Thermodynamics of Two-Dimensional Ideal Ferromagnets — Three-Loop Analysis*, *Phys. Rev. B* **86** (2012) 184409 [arXiv:1207.5937] [INSPIRE].

JHEP02(2025)092

[29] U. Gerber et al., *Constraint Effective Potential of the Staggered Magnetization in an Antiferromagnet*, *J. Stat. Mech.* **0903** (2009) P03021 [arXiv:0901.0445] [INSPIRE].

[30] O. Bar, M. Imboden and U.J. Wiese, *Pions versus magnons: from QCD to antiferromagnets and quantum Hall ferromagnets*, *Nucl. Phys. B* **686** (2004) 347 [cond-mat/0310353] [INSPIRE].

[31] F. Kampfer, M. Moser and U.-J. Wiese, *Systematic low-energy effective theory for magnons and charge carriers in an antiferromagnet*, *Nucl. Phys. B* **729** (2005) 317 [cond-mat/0506324] [INSPIRE].

[32] C. Brugger et al., *Two-Hole Bound States from a Systematic Low-Energy Effective Field Theory for Magnons and Holes in an Antiferromagnet*, *Phys. Rev. B* **74** (2006) 224432 [cond-mat/0606766] [INSPIRE].

[33] C. Brugger et al., *On the condensed matter analog of baryon chiral perturbation theory*, *AIP Conf. Proc.* **1116** (2009) 356 [INSPIRE].

[34] U.-J. Wiese, *Effective theories for magnetic systems*, *PoS* **CD09** (2009) 072 [INSPIRE].

[35] S. Chandrasekharan, F.-J. Jiang, M. Pepe and U.-J. Wiese, *Rotor Spectra, Berry Phases, and Monopole Fields: From Antiferromagnets to QCD*, *Phys. Rev. D* **78** (2008) 077901 [cond-mat/0612252] [INSPIRE].

[36] N.D. Vlasii and U.-J. Wiese, *Rotor Spectra and Berry Phases in the Chiral Limit of QCD on a Torus*, *Phys. Rev. D* **97** (2018) 114029 [arXiv:1803.06158] [INSPIRE].

[37] M. Beneke and V.A. Smirnov, *Asymptotic expansion of Feynman integrals near threshold*, *Nucl. Phys. B* **522** (1998) 321 [hep-ph/9711391] [INSPIRE].

[38] M. Lüscher, P. Weisz and U. Wolff, *A numerical method to compute the running coupling in asymptotically free theories*, *Nucl. Phys. B* **359** (1991) 221 [INSPIRE].

[39] G. Leibbrandt and J. Williams, *Split dimensional regularization for the Coulomb gauge*, *Nucl. Phys. B* **475** (1996) 469 [hep-th/9601046] [INSPIRE].

[40] F. Niedermayer and P. Weisz, *Matching effective chiral Lagrangians with dimensional and lattice regularizations*, *JHEP* **04** (2016) 110 [arXiv:1601.00614] [INSPIRE].

[41] J. Honerkamp and K. Meetz, *Chiral-invariant perturbation theory*, *Phys. Rev. D* **3** (1971) 1996 [INSPIRE].

[42] F. Niedermayer and P. Weisz, *Massless sunset diagrams in finite asymmetric volumes*, *JHEP* **06** (2016) 102 [arXiv:1602.03159] [INSPIRE].

[43] H. Bateman and A. Erdelyi, *Higher transcendental functions*, vol. I–III, Dover Publications (2006).

JHEP02(2025)092